HEART DISEASE

Hematopoietic loss of Y chromosome leads to cardiac fibrosis and heart failure mortality

Soichi Sano[1,2]*, Keita Horitani[1], Hayato Ogawa[1]†, Jonatan Halvardson[3], Nicholas W. Chavkin[1,4], Ying Wang[1]‡, Miho Sano[1]§, Jonas Mattisson[3], Atsushi Hata[5], Marcus Danielsson[3], Emiri Miura-Yura[1], Ammar Zaghlool[3], Megan A. Evans[1], Tove Fall[6], Henry N. De Hoyos[1], Johan Sundström[7]¶, Yoshimitsu Yura[1]†, Anupreet Kour[1], Yohei Arai[1], Mark C. Thel[1], Yuka Arai[1], Josyf C. Mychaleckyj[8], Karen K. Hirschi[4], Lars A. Forsberg[3,9]*, Kenneth Walsh[1]*

Hematopoietic mosaic loss of Y chromosome (mLOY) is associated with increased risk of mortality and age-related diseases in men, but the causal and mechanistic relationships have yet to be established. Here, we show that male mice reconstituted with bone marrow cells lacking the Y chromosome display increased mortality and age-related profibrotic pathologies including reduced cardiac function. Cardiac macrophages lacking the Y chromosome exhibited polarization toward a more fibrotic phenotype, and treatment with a transforming growth factor β1–neutralizing antibody ameliorated cardiac dysfunction in mLOY mice. A prospective study revealed that mLOY in blood is associated with an increased risk for cardiovascular disease and heart failure–associated mortality. Together, these results indicate that hematopoietic mLOY causally contributes to fibrosis, cardiac dysfunction, and mortality in men.

The human male-specific Y chromosome is relatively small in size and contains a limited number of genes that regulate sex determination and spermatogenesis (*1*). Beyond sex determination, there is a paucity of information about the biological role of the Y chromosome, partly because of challenges in determining genetic variation caused by the inter- and intrachromosomal repeat sequences. However, insights into the physiological role of the Y chromosome can be aided by studies that address the mosaic loss of chromosome Y (mLOY) in the blood, a condition in which a fraction of hematopoietic cells display a loss of the Y chromosome. This phenomenon is the most prevalent post-zygotic mutation in leukocytes (*2*). The frequency of hematopoietic mLOY increases with age and smoking status (*3*, *4*) and is associated with the condition of clonal hematopoiesis of indeterminate potential (CHIP) (*5*, *6*). Although the technology to assess mLOY is evolving, it has recently been reported that mLOY is detectable in 40% of 70-year-old males and 57% of 93-year-old males (*4*, *7*). Loss of the Y chromosome is prevalent in hematologic malignancies and may be a factor in the prognosis of these diseases. Whereas most men with mLOY never progress to a hematologic cancer, epidemiological studies have shown that mLOY in blood is associated with shorter life span (*2*, *8*) and increased incidence of various age-associated diseases, including solid tumors and Alzheimer's disease (*2*, *9*). Furthermore, mLOY has previously been associated with secondary major cardiovascular events in atherosclerotic patients after carotid endarterectomy (*10*) and with prior heart attack and stroke self-reported at baseline in the UK Biobank study (*8*). It has been reported that mLOY is in part a manifestation of inherited genomic instability and a marker of biological aging (*4*). However, because of the descriptive nature of epidemiological studies, it is unknown whether mLOY plays a causal role in disease development. Here, we modeled hematopoietic mLOY in mice and examined its role in fibrosis and cardiac dysfunction. Together with these results, prospective analyses of UK Biobank data suggest that mLOY in leukocytes directly contributes to heart failure.

[1]Hematovascular Biology Center, Robert M. Berne Cardiovascular Research Center, University of Virginia School of Medicine, Charlottesville, VA 22908, USA. [2]Department of Cardiovascular Medicine, Osaka Metropolitan University Graduate School of Medicine, Osaka 545-8585, Japan. [3]Department of Immunology, Genetics and Pathology, Science for Life Laboratory, Uppsala University, 75108 Uppsala, Sweden. [4]Department of Cell Biology, University of Virginia School of Medicine, Charlottesville, VA 22908, USA. [5]Chiba University Graduate School of Medicine, Department of General Thoracic Surgery, Chiba 260-8670, Japan. [6]Department of Medical Sciences, Molecular Epidemiology and Science for Life Laboratory, Uppsala University, 75185 Uppsala, Sweden. [7]Department of Medical Sciences, Uppsala University, Sweden, and Uppsala Clinical Research Center, 78185 Uppsala, Sweden. [8]Center for Public Health Genomics, University of Virginia, Charlottesville, VA 22908, USA. [9]The Beijer Laboratory, Uppsala University, 75185 Uppsala, Sweden.
***Corresponding author. Email: sano.soichi@omu.ac.jp (S.S.); lars.forsberg@igp.uu.se (L.A.F.); kw9ar@virginia.edu (K.W.)**
†Present address: Department of Cardiology, Nagoya University Graduate School of Medicine, Nagoya 466-8550, Japan.
‡Present address: Department of Cardiology, Xinqiao Hospital, Army Medical University, Chongqing 400037, China.
§Present address: Department of Obstetrics and Gynecology, Osaka Metropolitan University Graduate School of Medicine, Osaka 545-8585, Japan.
¶Present address: The George Institute for Global Health, University of New South Wales, Newtown, New South Wales 2042, Australia.

Results

Age-related pathologies are accelerated in mice with mLOY in blood

We constructed a mouse model of hematopoietic mLOY by using CRISPR-Cas9 gene editing to target repeat DNA sequences that are specific to the centromere of the Y chromosome. Guide RNAs (gRNAs) and a tomato red fluorescent protein (tRFP) marker were delivered to lineage-negative bone marrow cells through the lentivirus vector before transplantation into lethally irradiated, wild-type male mice (Fig. 1A). To decouple the *Cas9* gene from the lentivirus vector and to maximize gene-editing efficiency, donor bone marrow cells were isolated from ROSA26-Cas9 knock-in mice that express the Cas9 endonuclease systemically (*11*). Two LOY-gRNAs, LOY-gRNA1 and LOY-gRNA2, targeting different repeat sequences within the centromere were evaluated for the efficiency of Y chromosome ablation by fluorescent in situ hybridization (FISH) analysis of X and Y chromosomes in tRFP$^+$ blood cells collected from mice reconstituted with bone marrow cells. As a control, we used a lentivirus encoding a gRNA designed to not target any region of the genome in the ROSA26-Cas9 knock-in donor cells. Y chromosome ablation efficiency was ~95 and 80% for LOY-gRNA1 and LOY-gRNA2, respectively (Fig. 1, B and C). Thus, unless otherwise indicated, the mouse model of mLOY used a lentivirus vector that expresses the LOY-gRNA1 transcript and the tRFP$^+$ marker protein to assess cell transduction. Y chromosome ablation in vivo was validated by karyotype analysis using lineage-negative bone marrow cells isolated from mLOY and control mice that were immortalized by lentivirus-mediated HoxB8 overexpression (Fig. 1D). Consistent with the ablation of the male sex chromosome, the Y chromosome–encoded transcripts *Kdm5d*, *Uty*, *Eif2s3y*, and *Ddx3y* were not detectable in the circulating tRFP$^+$ leukocytes of the mLOY mice (Fig. 1E). Because of the inefficiency of bone marrow progenitor cell transduction by the lentivirus vector, blood chimerism, defined as a percentage of tRFP$^+$ white blood cells, ranged from 49 to 81% in various experiments (mean = 64.9 ± 4.0%), which is consistent with the levels of mLOY in men that have been associated with various disease processes (*2*, *9*). These levels of chimerism were maintained for 12 months (fig. S1A). Focusing on each immune cell population, chimerism was higher in myeloid cells compared with B and T cells, consistent with observations of mLOY in men (*12*) (fig. S1B).

The phenotypic consequences of mLOY were evaluated in aging male mice. No obvious hematological abnormalities were observed in mLOY or control mice during the follow-up period (fig. S1C). However, mice with the mLOY condition displayed shorter life spans compared with control mice (Fig. 1F). Serial echocardiographic analyses revealed the development of an accelerated age-associated cardiomyopathy in the mLOY mice, with greater

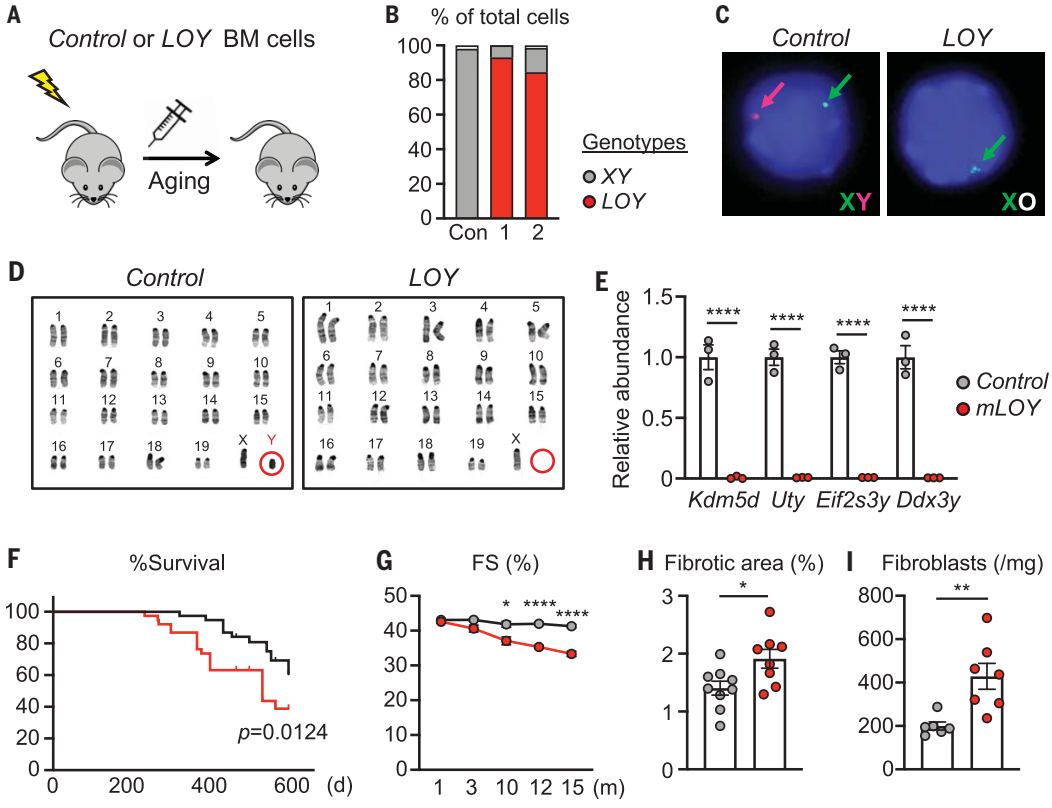

Fig. 1. Y chromosome deficiency in hematopoietic cells shortens life span and accelerates age-related cardiac dysfunction. (**A**) Schematic of this study. Lethally irradiated male C57BL6/J mice were reconstituted with hematopoietic stem cells transduced with lentivirus encoding Y chromosome targeting gRNA (LOY-gRNA) or control gRNA and designated as mLOY and control mice, respectively. Phenotypic differences between mLOY and control mice during the natural aging process were analyzed. (**B**) Efficiency of Y chromosome ablation analyzed by FISH. tRFP^{+} peripheral blood cells were collected from mice reconstituted with bone marrow cells transduced with lentivirus encoding a control gRNA or either of two different LOY-gRNAs: LOY-gRNA1 or LOY-gRNA2. The percentages of Y chromosome–deficient (LOY) cells and Y chromosome–sufficient cells (XY) in total blood cells are shown. Approximately 200 cells were analyzed for each condition. Unless otherwise indicated, all subsequent studies were performed with hematopoietic stem cells transduced with LOY-gRNA1. (**C**) Representative images of FISH analysis of peripheral blood cells collected from mLOY and control mice. Green and red fluorescence indicate the X and Y chromosomes, respectively. (**D**) Karyotype analysis of LOY and control cells. Hematopoietic stem cells collected from mLOY and control mice were immortalized by lentivirus-mediated HoxB8 transduction and subjected to karyotype analysis. (**E**) mRNA expression of genes on the Y chromosome in RFP^{+} peripheral blood leukocytes in mLOY and control mice (n = 3 per group). (**F**) Kaplan-Meier survival curve for mLOY and control mice after BMT. The x axis indicates time after BMT (day) (control, n = 37; mLOY, n = 38). (**G**) Sequential echocardiographic analysis of mLOY and control mice after BMT at the indicated time points (month) (n = 8 to 10 per group). (**H**) Quantitative analysis of fibrotic area in heart section at 15 months after BMT (n = 8 to 9 per group). (**I**) Flow cytometric analysis of fibroblast counts in heart tissue at 15 months after BMT (n = 6 to 7 per group). The absolute numbers of cells were normalized by tissue weight. Dots in all panels represent individual samples. Data are shown as mean ± SEM. Statistical analyses were performed using unpaired Student's t test [(E) and (H)], Student's t test with Welch's correction (I), log-rank test (F), and two-way repeated-measures ANOVA with Sidak's multiple-comparisons tests (G). FS, fractional shortening; RFP; red fluorescent protein, Con; control. *P < 0.05, **P < 0.01, ****P < 0.0001.

cardiac dysfunction detected in older mice (Fig. 1G and fig. S2A). Consistent with the development of an age-associated cardiomyopathy, mLOY mice displayed a small increase in heart mass at the termination of the experiment, but there were no differences in body weights between the mLOY and control genotypes over the course of the experiment (fig. S2B). The mLOY condition led to an increase in myocardial fibrotic area (Fig. 1H), as determined by quantitative analysis with picrosirius red staining of cardiac sections (fig. S2C), and an increase in the quantity of myocardial MEF-SK4^{+} fibroblasts, as assessed by flow cytometry (Fig. 1I). Consistent with this fibrotic response, the mLOY condition also led to increased left ventricular filling pressure, which is indicative of diastolic dysfunction (fig. S2D). These cardiac changes were observed despite modest reductions in blood pressure in the mLOY mice (fig. S2E) and no changes in the serum concentrations of renin 1 and angiotensin II (fig. S2F). Although further analyses of how mLOY affects the renin-angiotensin system are warranted, these experimental results are consistent with observations of diminished self-reported hypertension in cardiovascular disease patients with mLOY (*10*). At the 15-month time point after bone marrow transplantation (BMT), mLOY mice also showed accelerated fibrotic response in the lung interstitium (fig. S3A), and greater pulmonary fibrosis could also be observed in young mice after the intratracheal administration of bleomycin (fig. S3B). Histological analysis of the kidneys also revealed a greater degree of fibrosis in the mLOY mice compared with control mice at 15 months after BMT (fig. S3C). Finally, assessments of cognitive function revealed that aging mLOY mice (15 months after BMT) had short-term working memory deficits in the Y-maze and novel object recognition tests, but these phenotypes were not observed in young mLOY mice (2 months after BMT) (fig. S4). Collectively, these results indicate that mLOY mice can recapitulate aspects of the mLOY phenotype observed in men and suggest that accelerated tissue fibrosis could be a mechanistic feature of this condition. Because a potential relationship between mLOY and cardiac dysfunction has not been reported previously, further investigations focused on the role of mLOY in heart failure are warranted.

mLOY is associated with death from cardiovascular disease and heart failure in men

mLOY has been associated with preexisting cardiovascular disease (*8*, *10*). However, a prospective analysis of mLOY with mortality from cardiovascular disease with substantial follow-up time is lacking. Thus, we investigated male survival data extracted from the UK Biobank in November 2020 (median follow-up time, 11.5 years) and conducted three different types of analysis to evaluate whether mLOY in leukocytes was associated with risk for death

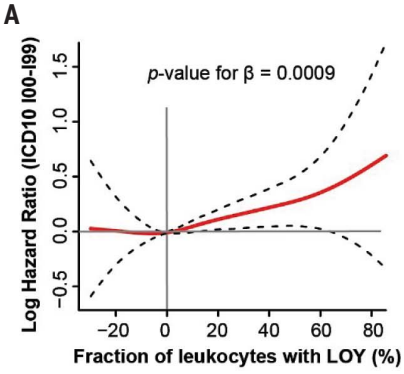

B

Cause of death	ICD10	n	HR (95% CI)	Adj. *p*-val.
All causes	A00-U99	15743	1.41 (1.20-1.65)	<0.0001
Diseases of the circulatory system	I00-I99	6222	1.31 (1.02-1.70)	0.0382
Hypertensive heart disease	I11	294	3.48 (1.54-7.89)	0.0028
Heart failure	I50	997	1.76 (1.01-3.05)	0.0446
Congestive heart failure	I50.0	381	2.42 (1.14-5.15)	0.0214
Aortic aneurysm and dissection	I71	227	2.76 (1.21-6.29)	0.0154

Fig. 2. Mosaic LOY in leukocytes is associated with all-cause mortality and death caused by cardiovascular diseases in men. (**A**) Results from the primary multivariable-adjusted Cox proportional hazards regression for mLOY and mortality from diseases of the circulatory system (ICD10 codes I00 to I99) modeled with a penalized spline approach and mLOY as a continuous variable. The solid red line represents the strength of association over the spectra of LOY mosaicism, and the dotted black lines denote the 95% confidence limits of the model. A linear regression analysis supported a positive slope of the association (*P* value for β = 0.0009). The analyzed dataset was extracted from the UK Biobank with an average follow-up time of 11.5 years, and the model was adjusted for confounding effects from age, smoking, alcohol consumption, body mass index, ancestry, blood pressure, total cholesterol, and diabetes. (**B**) Results from exploratory analyses using analogous multivariable adjusted Cox models with mLOY as a binary variable (at a 40% threshold). Shown are results from analyses of all-cause mortality (ICD10 codes A00 to U99), all diseases of the circulatory system (ICD10 codes I00 to I99), as well as specific cardiovascular causes of death with at least 200 events and significant association with mLOY at the 0.05 α level. *n*, number of events.

caused by cardiovascular diseases. The percentage of blood cells lacking chromosome Y in each male participant at baseline was estimated using intensity data from single-nucleotide polymorphism array experiments (fig. S5 and table S1). In the first analysis, a continuous estimate of mLOY was used as an explanatory variable in a multivariable-adjusted Cox proportional hazards regression for mLOY and death caused by cardiovascular disease, adjusted for the confounding variables outlined in table S2. The dependent variable in this primary model was mortality from any cardiovascular disease during follow-up, as indicated by a registered primary or secondary cause of death from the 10th revision of the International Statistical Classification of Diseases and Related Health Problems (ICD10) codes I00 to I99. This survival analysis established that mLOY in leukocytes is associated with death from overall cardiovascular disease in men [hazard ratio (HR) = 1.0054 per 1% increase in LOY, 95% confidence interval (CI) = 1.0022 to 1.0087, adjusted *P* = 0.0010, events = 6222). Using a penalized splines approach, the association could be illustrated over the full spectrum of LOY mosaicism (Fig. 2A), and a dose-response relationship was observed, indicating that mLOY might have a direct physiological effect. Exploratory Cox models using a binary LOY variable (defined from the spline analysis as described in fig. S6A) showed that men with LOY in >40% of leukocytes at study entry displayed 31% increased risk of dying from any disease of the circulatory system during follow-up (Fig. 2B, HR = 1.31, 95% CI = 1.02 to 1.70, adjusted *P* = 0.0382, events = 6222). To identify the specific cardiovascular outcomes that might be driving the overall association, we next investigated associations between mLOY and each of the ICD10 codes within I00 to I99 and with at least 200 observed events using analogous Cox models (table S3). The specific causes of death associated with mLOY included hypertensive heart disease (I11; HR = 3.48), heart failure (I50; HR = 1.76), congestive heart failure (I50.0; HR = 2.42), and aortic aneurysm and dissection (I71; HR = 2.76) (Fig. 2B). Because comorbidities are common among cardiovascular conditions, other registered cardiovascular-related causes of death showing association with mLOY (but normally not considered as primary causes of death) are summarized in fig. S6B. Next, cardiovascular diseases pooled on the basis of medical features and clinical resemblance were investigated using analogous survival models (table S4). In these extended analyses, there was no significant association between mLOY and death from diseases encompassing multiple etiologies of heart failure (HR = 1.65, 95% CI = 0.95 to 2.86, adjusted *P* = 0.0745, events = 1102). However, mLOY was associated with death caused by associated aortic and peripheral arterial diseases (HR = 2.79, 95% CI = 1.30 to 5.97, adjusted *P* = 0.0082, events = 279). Finally, corroborating prior analyses from the UK Biobank that used a shorter median (7-year) follow-up period (*8*), it was found that men with mLOY in >40% of leukocytes at study entry displayed a 41% increased risk of dying from any cause during the follow-up (Fig. 2B).

mLOY worsens the outcome of experimental heart failure in mice

To further investigate the relationship between mLOY and cardiac dysfunction, 12- to 16-week-old (4 weeks after BMT) male mice were subjected to transverse aortic constriction (TAC) surgery (Fig. 3A). Although TAC in mice does not completely replicate nonischemic heart failure, this widely used model produces cardiac dysfunction, left ventricle hypertrophy, and fibrosis phenotypes that are prevalent in the elderly (*13*). In agreement with observations in the older unchallenged mice, echocardiographic analysis revealed a greater progressive decline in cardiac function in mLOY mice compared with control mice after TAC (Fig. 3B and fig. S7A). The mLOY mice also displayed a marginally greater increase in the ratio of heart weight to tibia length, as well as an increase in the ratio of lung weight to tibia length that is indicative of lung congestion resulting from cardiac dysfunction (Fig. 3C). Transcripts encoding atrial natriuretic peptide A and the ratio of transcripts encoding myosin heavy chains β/α, a marker of advanced heart failure, were up-regulated in the hearts from mLOY mice compared with those from control mice (Fig. 3D). Histological analysis revealed greater interstitial and perivascular fibrosis in both the left ventricle and atrium of mLOY mice after TAC (Fig. 3E and fig. S7, B and C). Consistent with the increase in fibrosis, flow cytometric analysis of heart cells revealed that the number of MEF-SK4^{+} fibroblasts was higher in the hearts from TAC-treated mLOY mice compared with control (Fig. 3F). By contrast, there was no detectable difference in the number of cardiac endothelial cells or the average myocyte cross-sectional area between the experimental groups that had undergone TAC (Fig. 3, G and H), indicating that the predominant cellular effect of mLOY is on the fibroblast content of the heart.

Accelerated cardiac dysfunction could also be demonstrated in mice transplanted with lineage-negative bone marrow cells that were transduced with a gRNA that targets a different centromeric repeat in the Y chromosome (mLOY-gRNA2). The efficiency of

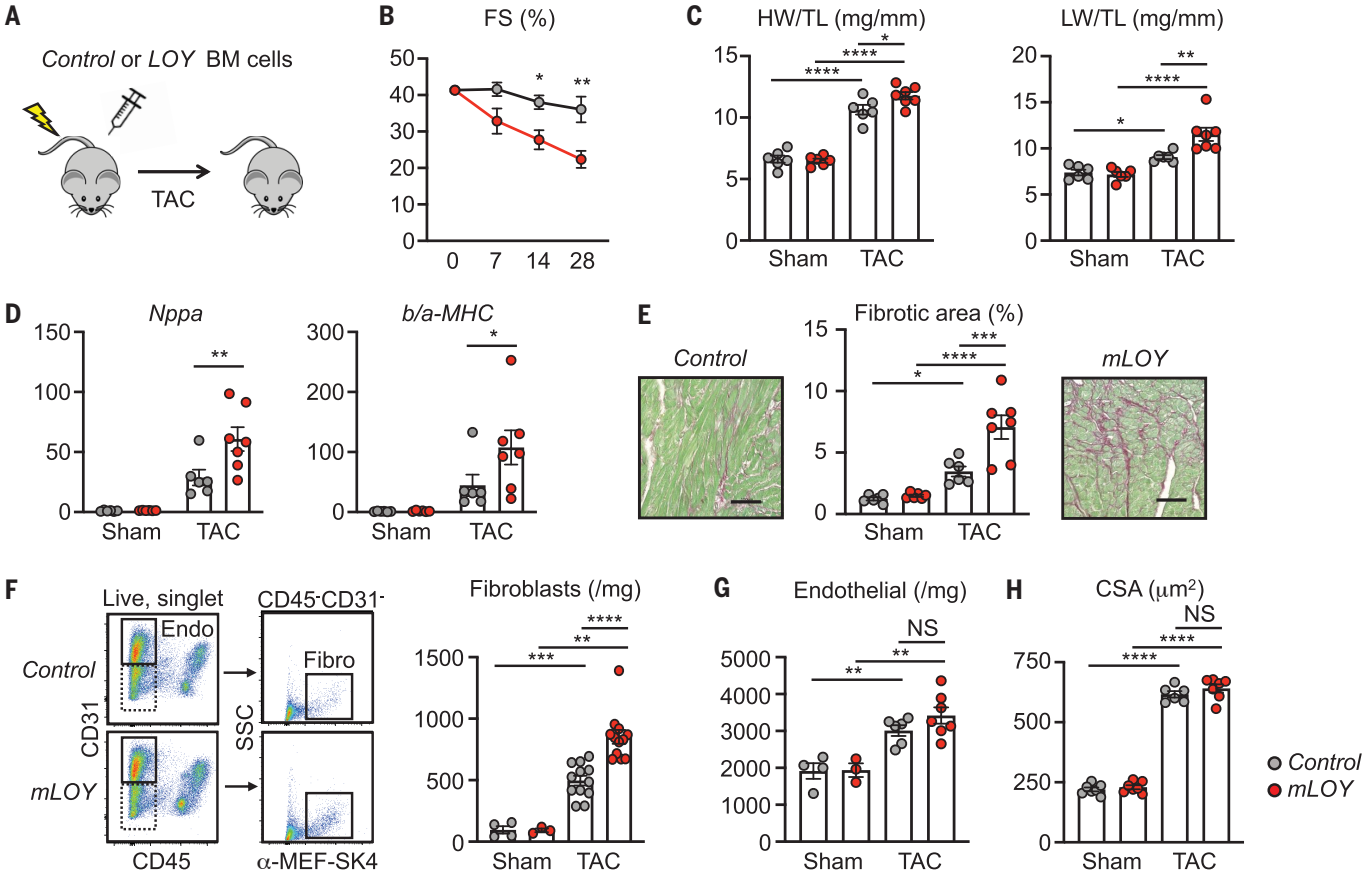

Fig. 3. Y chromosome deficiency in hematopoietic cells accelerates cardiac dysfunction in response to pressure overload. (**A**) Schematic of experimental study for assessing cardiac dysfunction of mLOY mice in the pressure overload model. mLOY mice were generated using LOY-gRNA1. At 4 weeks after BMT, mLOY mice or control mice were subjected to TAC. (**B**) Sequential echocardiographic analysis of mLOY and control mice after TAC at the indicated time points (control, $n = 6$; LOY, $n = 7$). (**C**) Heart weight (HW) and lung weight (LW) relative to tibial length (TL) in control sham mice and mice 4 weeks after TAC (control sham, $n = 6$; control mLOY, $n = 6$; control TAC, $n = 6$; mLOY TAC, $n = 7$). (**D**) Gene expression of the heart failure markers *Nppa* and *b/a-MHC* in heart tissue in sham mice and mice 4 weeks after TAC (control sham, $n = 6$; control mLOY, $n = 6$; control TAC, $n = 6$; mLOY TAC, $n = 7$). (**E**) Representative images and quantitative analysis (control sham, $n = 6$; control mLOY, $n = 6$; control TAC, $n = 6$; mLOY TAC, $n = 7$) of fibrotic area in heart sections in sham and 4-week after TAC. Scale bar, 100 μm. (**F** and **G**) Flow cytometric analysis of fibroblast (F) and endothelial cell (G) counts in heart tissue in sham mice and mice 4 weeks after TAC. Fibroblasts and endothelial cells are defined as $CD45^-CD31^-MEF\text{-}SK4^+$ and $CD45^-CD31^+$, respectively. The absolute numbers of cells were normalized by tissue weight ($n = 3$ to 4 per group in sham mice; $n = 6$ to 12 per group in TAC mice). (**H**) Mice with mLOY show comparable hypertrophic response of cardiac myocytes after TAC. Quantitative analysis of cross-sectional area of myocytes (CSA) in heart section at 4 weeks after TAC ($n = 6$ to 7 per group). Dots in all panels represent individual samples. Data are shown as mean ± SEM. Statistical analyses were performed using two-way repeated-measures ANOVA with Sidak's multiple-comparisons tests (B). Statistical analyses were performed using two-way ANOVA with Tukey's multiple-comparisons tests [(C), (D), (E), (F), and (G). $^*P < 0.05$, $^{**}P < 0.01$, $^{***}P < 0.001$, $^{****}P < 0.0001$.

Y chromosome ablation achieved by mLOY-gRNA2 was comparable but slightly less than that of mLOY-gRNA1 (Fig. 1B and fig. S8A). Transduction with mLOY-gRNA2 did not affect white blood cell counts, hemoglobin, or platelet counts (fig. S8B). However, TAC led to greater cardiac dysfunction, increased heart and lung weights, higher concentrations of serum brain natriuretic peptide (BNP), and higher numbers of cardiac fibroblasts in the mLOY-gRNA2–treated mice compared with control mice (fig. S8, C to F). These data corroborate the results with the mLOY-gRNA1 reagent and provide additional support for the finding that Y chromosome deletion in blood cells contributes to cardiac dysfunction and an accelerated fibrotic response.

Y chromosome deficiency modulates the transcriptional profile of cardiac macrophages

Myeloid cells typically display the greatest extents of Y chromosome deficiency in the blood of men (*12*). In the experimental model, analysis of the cardiac immune cell populations revealed higher numbers of $CCR2^+$ cardiac macrophages in TAC-treated hearts from mLOY-gRNA1 mice compared with those from control mice (fig. S9A), suggesting that cardiac macrophages derived from Y chromosome–deficient hematopoietic stem cells have altered functional properties. To test whether Y chromosome deficiency in myeloid cells accounts for the accelerated heart failure phenotype, anti–granulocyte receptor-1 (anti–GR-1) antibody, which blocks neutrophil and monocyte recruitment to injured tissue (*14*), was administered to the different experimental groups of mice. In mLOY mice that underwent TAC, treatment with anti–GR-1 antibody attenuated the accelerated cardiac dysfunction (fig. S9B) and reversed the elevations in heart weight and serum BNP (fig. S9, C and D). Treatment with anti–GR-1 antibody also reversed the increase of the number of cardiac fibroblasts observed in the mLOY mice, but it did not affect the quantity of vascular endothelial cells (fig. S9E). Collectively, these results suggest that loss of the Y chromosome in myeloid cells can largely account for the pathological cardiac phenotype in the mLOY mouse model.

To address the mechanistic aspects of mLOY-mediated cardiac dysfunction, single-cell RNA

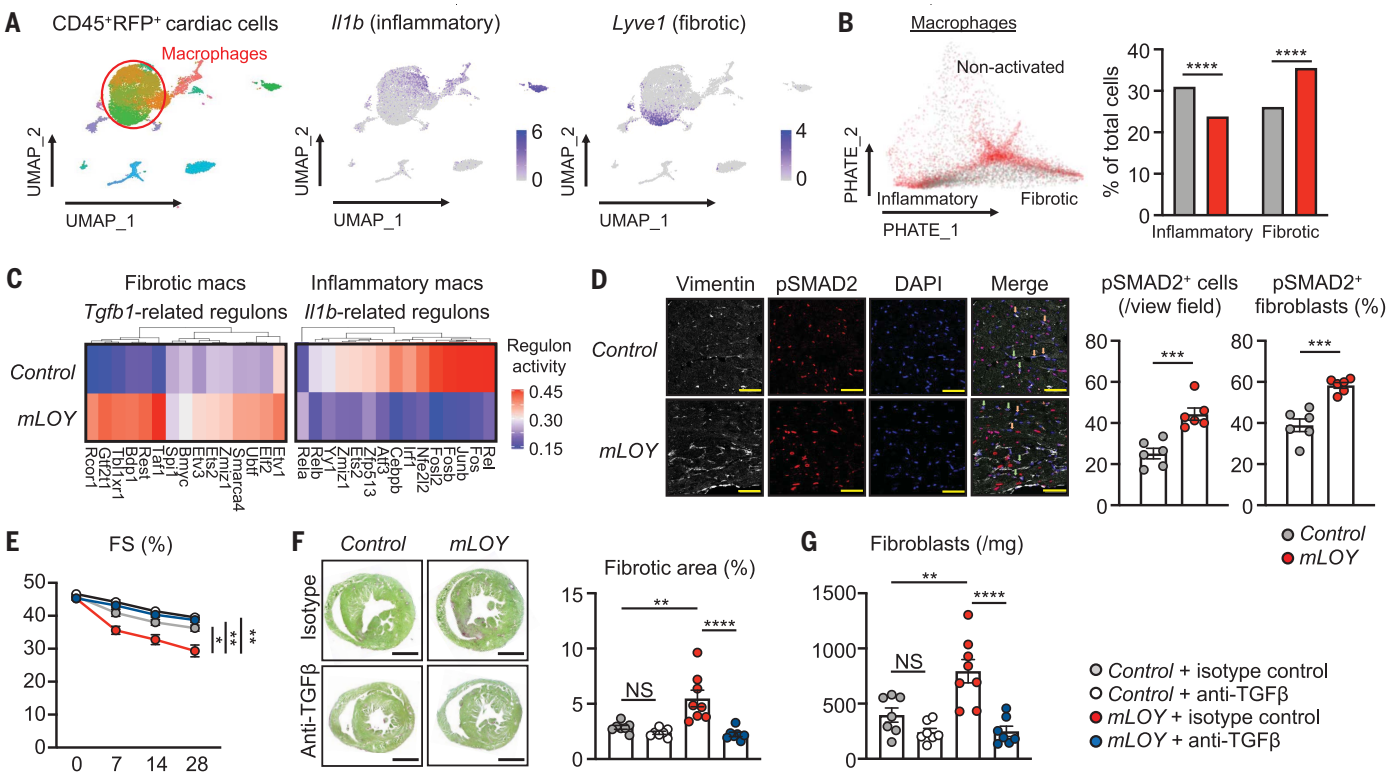

Fig. 4. Inhibition of TGFβ1 reverses cardiac dysfunction in mLOY mice after TAC. (**A**) Single-cell RNA sequencing from CD45^{+}RFP^{+} cardiac cells 7 days after TAC shown by uniform manifold approximation and projection (UMAP) dimensionality reduction, with inflammatory and fibrotic macrophages and expression of *Il1b* and *Lyve1* highlighted. (**B**) PHATE dimensionality reduction showing cells separated from control (gray) or mLOY (red) samples, with nonactivated, inflammatory, and fibrotic phenotypes labeled. Quantification of the relative percentage of control or mLOY cells contained in the inflammatory or fibrotic macrophage clusters. (**C**) Heatmap of transcription factor regulons within inflammatory or fibrotic macrophages related to *Il1b* or *Tgfb1* expression, respectively, that was generated using SCENIC analysis of control and mLOY cells. (**D**) Activation of TGFβ1 signaling in the heart accessed by immunofluorescent staining of phosphorylated SMAD2 (pSMAD2). The number of pSMAD2^{+} cells per view field and the percentage of pSMAD2^{+} fibroblasts (right) are shown. Fibroblasts are defined as vimentin^{+} cells (n = 6 fields per group). pSMAD2^{+} and pSMAD2^{-} fibroblasts are indicated by green and orange arrows, respectively. Scale bar, 50 μm. (**E**) At 4 weeks after BMT, mLOY mice or control mice were subjected to TAC. Anti-TGFβ1 antibody or isotype control was intraperitoneally injected every 3 days for 4 weeks. Shown is sequential echocardiographic analysis of mLOY and control mice after TAC operation at the indicated time points (n = 6 to 7 per group). (**F**) Representative images and quantitative analysis of fibrotic area in heart section at 4 weeks after TAC procedure (n = 6 to 8 per group). Scale bar, 1000 μm. (**G**) Flow cytometric analysis of fibroblast content in heart tissue at 4 weeks after TAC. The absolute numbers of cells were normalized by tissue weight (n = 7 to 8 per group). Dots in all panels represent individual samples. Data are shown as mean ± SEM. Statistical analyses were performed using chi-square test (B), unpaired Student's t test (D), two-way repeated-measures ANOVA with Sidak's multiple-comparisons test (E), and one-way ANOVA with Tukey's multiple-comparisons test [(F) and (G)]. *P < 0.05, **P < 0.01, ***P < 0.001, ****P < 0.0001.

sequencing was performed on BMT-derived (RFP^{+}) immune cells (CD45^{+}) from mLOY and control mice at 7 days after TAC. Seurat analysis of gene expression enabled the clustering of immune cell populations, and the reduced expression of Y chromosome–encoded genes could be detected in various clusters (fig. S10A). CD68^{+} macrophages accounted for the largest portion of immune cells, which displayed polarization based on the expression of the marker genes *Il1b* and *Ccr2*^{hi}, which will henceforth define an inflammatory subpopulation, and the marker genes *Lyve1* and *Mrc1*, which will henceforth define a fibrotic subpopulation (Fig. 4A and fig. S10B). PHATE (potential of heat diffusion for affinity-based trajectory embedding) analysis to assess differentiation progression and branching revealed a trajectory from nonactivated macrophages to a continuum of inflammatory and fibrotic macrophages (fig. S10C), with the fibrotic macrophage subpopulation containing a greater percentage of mLOY cells and the inflammatory macrophage subpopulation containing a greater percentage of control cells (Fig. 4B). Consistent with the interpretation that mLOY promotes macrophage polarization toward a fibrotic phenotype, analysis with the SCENIC (single-cell regulatory network inference and clustering) regulatory gene network algorithm revealed that profibrotic regulons were enriched by the mLOY condition in the fibrotic macrophages (fig. S10D). Conversely, proinflammatory regulons were suppressed by the mLOY condition in the inflammatory macrophage subpopulation. Further analyses revealed that the mLOY condition promoted the enrichment of regulons specifically associated with transforming growth factor–β1 (TGFβ1) signaling in the fibrotic macrophage subpopulation, whereas regulons associated with interleukin-1β (IL-1β) signaling were down-regulated by mLOY in the inflammatory subpopulation (Fig. 4C). The mLOY condition promoted the expression of the transcript encoding TGFβ1 in the fibrotic macrophages, but not in the inflammatory macrophages, whereas the transcript encoding galectin-3, another secreted profibrotic protein, was up-regulated by the mLOY condition in both macrophage populations (fig. S10E).

The phenotypic transition of Y chromosome–deficient cardiac macrophages was also evident in a bulk transcriptome analysis of BMT-derived

(RFP$^+$) cardiac macrophages. As shown in the principal components analysis plots, mLOY macrophages isolated from heart displayed a transcriptomic profile distinct from that of control cardiac macrophages (fig. S11A). Gene set enrichment analysis (GSEA) revealed that differentially expressed transcripts related to "TGFβ signaling" were enriched in mLOY macrophages (fig. S11B). In addition, GSEA revealed that differentially expressed transcripts related to "TGFβ binding," including LTBP1, LTBP3, LTBP4, and thrombospondin, which facilitate the localization, secretion, and activation of TGFβ1, as well as other profibrotic factors, were up-regulated in macrophages in the mLOY condition (fig. S11C). In marked contrast, bulk or single-cell analysis revealed little or no differences in transcriptomes of cardiac monocytes, cardiac neutrophils, or blood neutrophils between the mLOY and control conditions (fig. S11, D to G).

Consistent with the transcriptome analyses, elevated TGFβ1 protein and SMAD2 phosphorylation in the myocardium could be detected by immunoblot analysis in the mLOY condition compared with control at 1 week after TAC (fig. S12, A and B). Elevated TGFβ1 protein in the mLOY condition could also be detected by fluorescence immunohistochemistry (fig. S12C). Although TGFβ1/macrophage colocalization was found to a greater extent in the mLOY condition, most of the TGFβ1 signal was localized to other cell types or matrix in the myocardium, consistent with its putative role in a feedforward signaling loop and its affinity for extracellular matrix. Furthermore, the total number of phosphorylated SMAD2$^+$ cells was higher in mLOY mice compared with control mice at 1 week after TAC, as confirmed by quantitative analysis of phosphorylated SMAD2$^+$ fibroblasts identified by co-immunostaining with vimentin (Fig. 4D).

TGFβ1 neutralization reverses the cardiac dysfunction observed in mLOY mice

To assess the role of profibrotic signaling in accelerated cardiac dysfunction caused by the experimental mLOY condition, mice that had undergone TAC were treated with control immunoglobulin G or a monoclonal antibody directed toward TGFβ1. Sequential echocardiographic analysis revealed that treatment with anti-TGFβ1 monoclonal antibody partly reversed the accelerated cardiac dysfunction observed in mLOY mice (Fig. 4E and fig. S12D). The anti-TGFβ1 antibody also reversed the mLOY-mediated increases in serum BNP concentration, heart weight, and lung congestion (fig. S12, E and F). Consistent with the recognized functions of TGFβ1 in promoting fibroblast proliferation and their conversion to myofibroblasts that produce higher amounts of matricellular proteins, the neutralizing anti-TGFβ1 antibody suppressed the increase in fibroblast number and extracellular matrix deposition that was associated with the mLOY condition but did not alter endothelial cell number (Fig. 4, F and G, and fig. S12G).

Discussion

Tissue fibrosis is a hallmark of aging and is estimated to contribute to 45% of deaths in industrialized countries (*13*). Myocardial fibrosis results from the activation of cardiac-resident fibroblasts and is often associated with heart failure, a major cause of mortality and morbidity in the elderly. Myocardial fibrosis can be triggered by bone marrow–derived macrophages that acutely infiltrate the heart in response to various forms of cardiac injury or progressively replace the cardiac-resident, yolk sac–derived macrophages with age (*15*, *16*). Here, we provide evidence in mouse models that supports a causal link between hematopoietic mLOY and age-dependent cardiac dysfunction and heart failure in men. We report that Y chromosome–deficient cardiac macrophages overactivate a profibrotic signaling network, leading to cardiac fibroblast proliferation and activation, excessive matrix production, and diminished heart function. The observation of profibrotic signaling in mLOY is unexpected compared with findings of how CHIP mechanistically contributes to cardiovascular disease. Whereas there is a high co-occurrence of mLOY with CHIP (*5*, *6*), and both are associated with cardiovascular disease mortality, including heart failure (*17*, *18*), CHIP appears to largely promote pathological processes through the overactivation of IL-1β/IL-6 inflammatory signaling in myeloid cells (*19*–*22*). It is increasingly recognized that chronic diseases are caused by a spectrum of inflammation- and fibrosis-driven events (*23*). However, the interrelationship between inflammation and fibrosis is not simply reciprocal in that chronic inflammation will promote fibrosis, whereas fibrosis can function in the resolution of inflammatory processes. Thus, the somatic mosaicism that develops in the hematopoietic system with age may give rise to a complex interplay of pro- and anti-inflammatory processes that can differentially affect disease development. Finally, our experimental studies also found that a neutralizing TGFβ1 antibody could reverse the pathological cardiac phenotypes caused by mLOY. In view of recent efforts to treat heart failure, idiopathic pulmonary fibrosis, and some cancers with antifibrotic approaches (*24*–*27*), men with mLOY could represent a patient subpopulation that exhibits a superior response to this class of therapeutic agents.

REFERENCES AND NOTES

1. M. A. Jobling, C. Tyler-Smith, *Nat. Rev. Genet.* **18**, 485–497 (2017).
2. L. A. Forsberg *et al.*, *Nat. Genet.* **46**, 624–628 (2014).
3. J. P. Dumanski *et al.*, *Science* **347**, 81–83 (2015).
4. D. J. Thompson *et al.*, *Nature* **575**, 652–657 (2019).
5. V. Ljungström *et al.*, *Leukemia* **36**, 889–891 (2022).
6. F. Zink *et al.*, *Blood* **130**, 742–752 (2017).
7. L. A. Forsberg *et al.*, *Nat. Genet.* **51**, 4–7 (2019).
8. E. Loftfield *et al.*, *Sci. Rep.* **8**, 12316 (2018).
9. J. P. Dumanski *et al.*, *Am. J. Hum. Genet.* **98**, 1208–1219 (2016).
10. S. Haitjema *et al.*, *Circ. Cardiovasc. Genet.* **10**, e001544 (2017).
11. S. Sano *et al.*, *J. Vis. Exp.* (152): (2019).
12. J. P. Dumanski *et al.*, *Cell. Mol. Life Sci.* **78**, 4019–4033 (2021).
13. D. C. Rockey, P. D. Bell, J. A. Hill, *N. Engl. J. Med.* **372**, 1138–1149 (2015).
14. J. M. Daley, A. A. Thomay, M. D. Connolly, J. S. Reichner, J. E. Albina, *J. Leukoc. Biol.* **83**, 64–70 (2008).
15. A. J. Rhee, K. J. Lavine, *Annu. Rev. Physiol.* **82**, 1–20 (2020).
16. Y. Wang *et al.*, *JCI Insight* **5**, e135204 (2020).
17. L. Dorsheimer *et al.*, *JAMA Cardiol.* **4**, 25–33 (2019).
18. B. Yu *et al.*, *J. Am. Coll. Cardiol.* **78**, 42–52 (2021).
19. J. J. Fuster *et al.*, *Science* **355**, 842–847 (2017).
20. S. Sano *et al.*, *Circ. Res.* **123**, 335–341 (2018).
21. S. Sano *et al.*, *J. Am. Coll. Cardiol.* **71**, 875–886 (2018).
22. Y. Yura *et al.*, *Circ. Res.* **129**, 684–698 (2021).
23. M. Wijsenbeek, V. Cottin, *N. Engl. J. Med.* **383**, 958–968 (2020).
24. T. E. Kang Jr. *et al.*, *N. Engl. J. Med.* **370**, 2083–2092 (2014).
25. G. A. Lewis *et al.*, *Nat. Med.* **27**, 1477–1482 (2021).
26. A. Fujiwara *et al.*, *Sci. Rep.* **10**, 10900 (2020).
27. H. Aghajanian *et al.*, *Nature* **573**, 430–433 (2019).

ACKNOWLEDGMENTS

We thank the participants and enablers of the UK Biobank study. This research was conducted using the UK Biobank Resource under application no. 61272 and enabled by the University of Virginia Flow Cytometry Core (RRID: SCR_017829) and the Genome Analysis and Technology Core (RRID:SCR_018883). LV.T11.Hosb8.Puro was provided by R. Förster at Hannover Medical School. **Funding:** This work was supported by the National Institutes of Health (NIH grants AG073249, AG072095, HL141256, HL139819, and HL142650 to K.W.; NIH grant HL152174 to S.S. and K.W.; Grant-in-Aid for Research Activity Start-up 21K20879 to S.S.; Grant-in-Aid for Scientific Research C 22K08162 to S.S.; and NIH Grant HL146056 to K.K.H.); the MSD Life Science Foundation (S.S.); the Ichiro Kanehara Foundation (S.S.); the Kenzo Suzuki Memorial Foundation (S.S); YOKOYAMA Foundation for Clinical Pharmacology (S.S.); the Cardiovascular Research Fund (S.S.); The Japanese Heart Failure Society (S.S.); the Osaka Medical Research Foundation for Intractable Diseases (S.S.); The European Research Council (ERC) under the European Union's Horizon 2020 Research and Innovation Program (grants 679744 and 101001789 to L.A.F.); the Swedish Research Council (grant 2017-03762 to L.A.F.); The Swedish Cancer Society (grant 20-1004 to L.A.F.); Kjell och Märta Beijers Stiftelse (L.A.F.); Marcus Borgströms stiftelse (J.H.); and the American Heart Association (grant 20POST35210098 to M.A.E.). **Author contributions:** S.S., K.K.H., L.A.F., and K.W. designed the experiments. S.S., K.H., H.O., Y.W., M.S., A.H., E.M.-Y., M.A.E., H.N.D.H., Y.Y., A.K., N.W.C., Yo.A., M.C.T., Yu.A., and J.C.M. performed the experiments. J.H., J.M., M.D., A.Z., T.F., J.S., and L.A.F. analyzed the UK Biobank data. S.S., H.O., L.A.F., and K.W. wrote the paper. All authors contributed to editing the final version of the paper. **Competing interests:** L.A.F. is cofounder and shareholder of Cray Innovation AB. The remaining authors declare no competing interests. **Data and materials availability:** All data are available in the main text or the supplementary materials. Data were deposited into the National Center for Biotechnology Information's Gene Expression Omnibus database under accession numbers GSE205091 and GSE204732.

SUPPLEMENTARY MATERIALS

science.org/doi/10.1126/science.abn3100
Materials and Methods
Figs. S1 to S12
Tables S1 to S7
References (*28*–*30*)
MDAR Reproducibility Checklist

View/request a protocol for this paper from *Bio-protocol*.

Submitted 17 November 2021; accepted 6 June 2022
10.1126/science.abn3100